diffusion-fundamentals

The Open-Access Journal for the Basic Principles of Diffusion Theory, Experiment and Application

Multiple correlation function approach: rigorous results for simple geometries

D. S. Grebenkov

Laboratoire de Physique de la Matière Condensée, CNRS – Ecole Polytechnique, F-91128 Palaiseau, France

(received 1 May 2007, accepted 5 June 2007)

Abstract

The multiple correlation function approach is briefly presented and applied to investigate spin-echo signal attenuation due to restricted diffusion in simple geometries (slab, cylinder, and sphere) in the presence of surface relaxation. Exact and explicit representations for the zeroth and second moments of the total phase accumulated by diffusing spins are derived by using the Laplace transform summation technique. Within the Gaussian phrase approximation, these two moments determine the reference and diffusion-weighted signals, respectively. In the slow-diffusion or short-time regime, the series expansion in half-integer powers of the diffusion coefficient is generalized to arbitrary temporal profile of a linear magnetic field gradient. In the motional-narrowing or long-time regime, it is shown how the presence of surface relaxation modifies the classical Robertson's relation. Practical consequences of these findings are discussed.

Key words: magnetic resonance, restricted diffusion, confined media, surface relaxation
PACS: 76.60.-k, 82.56.Lz, 61.43.Gt, 76.60.Lz

1 Introduction

Restricted diffusion is a fundamental transport mechanism in many physical, chemical, biological and industrial systems. The presence of a geometrical confinement strongly influences the motion of diffusing species and the functioning of the system. This influence was experimentally observed in different fields, in particular, in nuclear magnetic resonance (NMR). In a typical spin-echo experiment, the combination of 90° and 180° radio-frequency (rf) pulses

Email address: denis.grebenkov@polytechnique.edu (D. S. Grebenkov).

Diffusion Fundamentals 5 (2007) 1.1 - 1.34

is used to excite and refocus the transverse magnetization of nuclei diffusing in an inhomogeneous magnetic field (e.g., a linear gradient g). The resulting spin-echo signal is formed by a large ensemble of the nuclei, each of which traveled a random trajectory and thus experienced different magnetic field intensities. Hahn, and later Carr and Purcell found the echo amplitude at time T for unrestricted diffusion in a steady linear gradient [1,2]

$$E \propto \exp\Big[-\gamma^2 g^2 T^3 D/12\Big], \tag{1}$$

γ being the nuclear gyromagnetic ratio, and D the free diffusion coefficient. When the motion of nuclei is restricted, the behavior is remarkably different. For a steady linear gradient, the signal attenuation was first predicted by Robertson and experimentally observed by Wayne and Cotts for restricted diffusion of methane gas between two parallel Teflon plates at distance L [3,4]

$$E \propto \exp\Big[-\gamma^2 g^2 T L^4/(120D)\Big]. \tag{2}$$

In particular, the signal is very sensitive to the size L of the geometrical confinement.

Since Robertson, many theoretical, numerical and experimental works dealt with restricted diffusion in simple confinements (see [5,6] for reviews). Neuman extended Robertson's result to a cylinder and a sphere [7], while Tarczon and Halperin considered nonlinear magnetic fields in a slab [8]. Stoller, Happer, and Dyson analyzed the spectral problem associated to the Bloch-Torrey equation on an interval [9]. Their predictions were confirmed by Hürlimann and co-workers who measured the signal attenuation due to diffusion of water protons between parallel glass coverplates [10].

In addition to gradient-induced dephasing, surface relaxation causes the magnetization loss and the consequent signal attenuation. Brownstein and Tarr considered restricted diffusion in the presence of surface relaxation in homogeneous magnetic fields (without linear gradient) [11]. Mitra and co-workers developed a mathematical theory to study the influence of surface relaxation on the effective diffusion coefficient $D(t)$ for pulsed-gradient spin-echo (PGSE) experiments [12–14]. The assumption of very narrow gradient pulses allowed them to deduce a number of analytical results. In particular, for isotropic smooth boundaries, they found in the short-time limit

$$\frac{D(t)}{D} = 1 - \frac{4}{3\sqrt{\pi}}\,\frac{S}{Vd}(Dt)^{1/2} + \frac{S}{3V}\left(\frac{\rho}{2} - \frac{H}{4}\right)(Dt) + O\Big[(Dt)^{3/2}\Big], \tag{3}$$

where ρ is the surface relaxivity, S/V is the surface-to-volume ratio, H is the mean curvature of the surface, and d is the dimension of space. This asymptotic expansion has been illustrated by analytical results for a sphere. de Swiet and Sen derived similar asymptotic relations for a steady linear gradient [15]. Experimental measurements of the time-dependent diffusion coefficient $D(t)$ were

Diffusion Fundamentals 5 (2007) 1.1 - 1.34

suggested to determine the surface-to-volume ratio and surface relaxation in porous media [16–18]. Coy and Callaghan investigated in detail restricted diffusion between parallel planes in PGSE experiments in the presence of surface relaxation, comparing theoretical, numerical and experimental results [19]. In addition, Callaghan gave explicit formulas for the PGSE signal attenuation for planar, cylindrical and spherical pores [20].

For efficient numerical investigation, several matrix formalisms have been developed. Caprihan and co-workers proposed a multiple-narrow-pulse approximation for restricted diffusion in a time-varying field gradient [21], while Callaghan reformulated it in an elegant matrix form [22,23]. An alternative approach was developed by Barzykin [24,25] and further extended by Axelrod and Sen [26] and by Grebenkov [6]. The latter extension was called "multiple correlation function" approach. This general mathematical technique allows the spin-echo signal and all the moments of the total dephasing to be expressed in terms of the eigenvalues and eigenfunctions of the Laplace operator in any confining domain (see below).

Except for the case of very narrow gradient pulses (PGSE experiment), analytical derivation of the signal attenuation in the presence of surface relaxation is a difficult task, even for simple geometries. Kuchel and co-workers first attempted extending the results of Robertson and Neuman to include surface relaxation for restricted diffusion in a sphere in a steady linear magnetic field gradient [27]. They expressed the analytical solution as an infinite series of spherical Bessel functions. However, the important condition ensuring the magnetization survival up to the echo time (see below) was not taken into account, leading to emergence of a (fictituous) second minimum in the signal dependence on the diffusion coefficient. This may serve as an illustration for the technical complexity of finding analytical solutions including surface relaxation.

In this paper, the multiple correlation function approach is used to derive rigorous results for restricted diffusion in simple geometries (slab, cylinder and sphere) in the presence of surface relaxation. As shown in [6], the symmetry of these domains implies that the spin-echo signal and all relevant characteristics are determined by the Laplace operator eigenvalues only. This is a crucial simplification of the problem that allows one to apply efficient analytical methods like a Laplace transform summation technique. Using this technique, we obtain an exact and explicit relation for the Laplace transform of the zeroth and second moments. In a typical situation of weak gradients, these moments determine the signal attenuation (so-called "Gaussian phase approximation"). We show how surface relaxation may influence the effective or apparent diffusion coefficient in the slow-diffusion and motional-narrowing regimes.

Diffusion Fundamentals 5 (2007) 1.1 - 1.34

The paper has twofold purpose. On the one hand, we demonstrate the facilities of using the multiple correlation function approach in theoretical studies. The choice of simple geometries allows one to perform the calculation analytically. In particular, the efficiency of the Laplace transform summation technique is illustrated. On the other hand, the classical relations of Robertson and Neuman are extended to include surface relaxation. Although the obtained formulas are specific for slab, cylinder, and sphere, their common features seem to be quite general.

The paper is organized as follows. In the next Section, a brief introduction to the multiple correlation function approach is given following Ref. [6]. The computation for three geometries (slab, cylinder, and sphere) is presented. In Sec. 3, we consider the slow-diffusion regime and describe the Laplace transform summation technique. Section 4 concerns the motional-narrowing regime. General discussion and physical applications of the derived mathematical results are presented in Sec. 5. Some technical issues are placed in the Appendixes.

2 Multiple correlation function approach

In this section, we briefly present the multiple correlation function approach following Ref. [6]. The historical background and further details can be found in that reference.

2.1 Total accumulated phase

In a typical spin-echo experiment, the combination of a 90° rf pulse at time 0 and of a 180° rf pulse at time $T/2$ is used to excite and refocus the transverse magnetization of nuclei, forming an echo at time T. For computational purpose, it is convenient to introduce dimensionless time $0 \leq t \leq 1$ by rescaling the time interval between 0 and T. We consider the magnetic field with a linear gradient in direction $\mathbf{e}_g$ and of the maximum intensity g. The time dependence of the gradient is represented via the normalized temporal profile $f(t)$, in which the magnetization sign change by the 180° rf pulse is effectively taken into account (Fig. 1). The temporal profile satisfies the rephasing condition so that the total accumulated phase of immobile nuclei would be 0:

$$\int_0^1 dt\ f(t) = 0.$$

Diffusion Fundamentals 5 (2007) 1.1 - 1.34

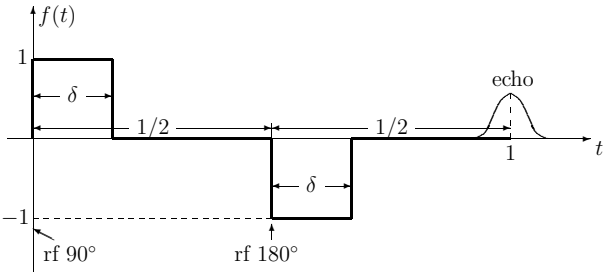

Fig. 1. Normalized temporal profile (shown by bold line) with two rectangular pulses of duration δ, where the magnetization sign change by the 180° rf pulse is effectively taken into account. One retrieves a steady (bipolar) gradient for $\delta = 1/2$.

In contrast, a diffusing nucleus experiences different magnetic field intensities and thus accumulates the total phase φ up to the echo time:

$$\varphi = (\gamma g L T) \int_0^1 dt \; f(t) \; B(X_t), \tag{4}$$

where $B(X_t)$ is the normalized projection of the spin trajectory X_t onto the gradient direction $\mathbf{e}_g$: $B(X_t) = (X_t \cdot \mathbf{e}_g)/L$, L being a characteristic size of the confining domain Ω. Since the diffusing nuclei are confined to remain in the domain, X_t is a random trajectory of the reflected Brownian motion [28]. The integral in Eq. (4) is thus a random variable, that we denote ϕ, and the coefficient $q = \gamma g L T$ in front of the integral is the dimensionless gradient intensity so that $\varphi = q\phi$.

A spin echo is formed by the whole ensemble of diffusing nuclei. The measured macroscopic signal appears then by averaging the transverse magnetization $e^{iq\phi}$ of each individual nucleus over the sample. Since the number of the nuclei is very large, one can replace this ensemble average by expectation over all possible Brownian trajectories:

$$E \propto \mathbb{E}\{\exp[iq\phi]\}. \tag{5}$$

In the presence of surface relaxation, the signal decays even without linear gradient. In practice, one usually normalize the above diffusion-weighted signal by so-called reference signal $E_0 \propto \mathbb{E}\{1\}$ without linear gradient ($q = 0$). For weak gradients ($q \ll 1$), the series expansion of Eq. (5) yields

$$E_{\text{norm}} \simeq \frac{\mathbb{E}\{1\} - q^2\mathbb{E}\{\phi^2/2\} + ...}{\mathbb{E}\{1\}} \simeq \exp\left[-q^2 \frac{\mathbb{E}\{\phi^2/2\}}{\mathbb{E}\{1\}}\right] \tag{6}$$

(assuming that the first moment vanishes). This relation is often called "Gaussian phase approximation" (GPA). In probabilistic language, the above ratio of the moments can be understood as conditional expectation over the nuclei

Diffusion Fundamentals 5 (2007) 1.1 - 1.34

whose magnetizations are survived up to the echo time. In what follows, we investigate this quantity in detail.

2.2 Zeroth moment

The attenuation of the spin-echo signal by surface relaxation without linear magnetic field gradient was first considered by Brownstein and Tarr [11]. This signal E_0 is formed by the diffusing nuclei whose transverse magnetization "survived" up to the echo time: $E_0 \propto \mathbb{E}\{1\}$. In probabilistic language, the zeroth moment represents the fraction of survived trajectories:

$$\mathbb{E}\{1\} = \int\limits_{\Omega} d\mathbf{r}_0 \; \rho_0(\mathbf{r}_0) \int\limits_{\Omega} d\mathbf{r}_1 \; G_1(\mathbf{r}_0, \mathbf{r}_1), \tag{7}$$

where $\rho_0(\mathbf{r}_0)$ is the initial density of the nuclei, and $G_t(\mathbf{r}, \mathbf{r}')$ is called the diffusive propagator, heat kernel, or, equivalently, Green's function of diffusion equation in the confining domain Ω. The above expression states that the signal is averaged over all spins started at time $t = 0$ at random position $\mathbf{r}_0$ (chosen with the probability $\rho_0(\mathbf{r}_0)d\mathbf{r}_0$) and arrived at time $t = 1$ to random position $\mathbf{r}_1$ (with the probability $G_1(\mathbf{r}_0, \mathbf{r}_1)d\mathbf{r}_1$).

It is convenient to introduce the orthonormal eigenfunctions $u_m(\mathbf{r})$ and the normalized eigenvalues λ_m of the Laplace operator, $\Delta = \partial^2/\partial x_1^2 + ... + \partial^2/\partial x_d^2$, in the confining domain Ω:

$$\Delta u_m + \frac{\lambda_m}{L^2} u_m = 0 \quad (\text{in } \Omega), \tag{8}$$

$$\frac{\partial u_m}{\partial n} + \frac{h}{L} u_m = 0 \quad (\text{on } \partial\Omega). \tag{9}$$

Here $\partial/\partial n$ is the outward normal derivative, and

$$h = \rho L/D$$

is the dimensionless surface relaxivity. The heat kernel can be expanded in a series over eigenfunctions

$$G_t(\mathbf{r}, \mathbf{r}') = \sum_{m=0}^{\infty} u_m(\mathbf{r}) \; u_m^*(\mathbf{r}') \; e^{-pt\lambda_m}, \tag{10}$$

where

$$p = DT/L^2$$

Diffusion Fundamentals 5 (2007) 1.1 - 1.34

is the dimensionless diffusion coefficient. The substitution of the above expansion in Eq. (7) yields

$$\mathbb{E}\{1\} = \sum_{m=0}^{\infty} U_m \; e^{-p\lambda_m} \; \tilde{U}_m^*,$$

where

$$U_m = V^{1/2} \int\limits_{\Omega} d\mathbf{r}_0 \; \rho_0(\mathbf{r}_0) \; u_m(\mathbf{r}_0),$$
$$\tilde{U}_m = V^{-1/2} \int\limits_{\Omega} d\mathbf{r}_1 \; u_m(\mathbf{r}_1),$$

V being the volume of the confining domain Ω. By introducing the infinite-dimensional diagonal matrix

$$\Lambda_{m,m'} = \delta_{m,m'} \lambda_m,$$

one can write the zeroth moment E_0 in the compact form of a scalar product:

$$\mathbb{E}\{1\} = \Big(U \; e^{-p\Lambda} \; \tilde{U}^* \Big).$$

2.3 Second moment

Similarly, the second moment can be explicitly written as a kind of time average $< ... >_2$ with a given normalized temporal profile $f(t)$ of the correction function $\mathbb{E}\{X_{t_1} X_{t_2}\}$:

$$\mathbb{E}\{\phi^2/2\} = < \mathbb{E}\{X_{t_1} X_{t_2}\} >_2 . \tag{11}$$

Here the time average of any function $F(t_1, t_2)$ is defined as

$$< F(t_1, t_2) >_2 = \int\limits_0^1 dt_1 \; f(t_1) \int\limits_{t_1}^1 dt_2 \; f(t_2) \; F(t_1, t_2), \tag{12}$$

while the correction function is

$$\begin{aligned} \mathbb{E}\{X_{t_1} X_{t_2}\} = & \int\limits_{\Omega} d\mathbf{r}_0 \; \rho_0(\mathbf{r}_0) \int\limits_{\Omega} d\mathbf{r}_1 \; G_{t_1}(\mathbf{r}_0, \mathbf{r}_1) \; B(\mathbf{r}_1) \; \times \\ & \int\limits_{\Omega} d\mathbf{r}_2 \; G_{t_2 - t_1}(\mathbf{r}_1, \mathbf{r}_2) \; B(\mathbf{r}_2) \int\limits_{\Omega} d\mathbf{r}_3 \; G_{1-t_2}(\mathbf{r}_2, \mathbf{r}_3). \end{aligned} \tag{13}$$

The last integral over $\mathbf{r}_3$ is required to ensure that the magnetization of the considered nucleus is not lost until the echo time. [1] Substitution of the series

[1] If there is no surface relaxation ($h = 0$), the last integral is simply equal to 1 due to the normalization of the heat kernel. When $h > 0$, the omission of this integral may lead to artifacts (see Ref. [27]).

Diffusion Fundamentals 5 (2007) 1.1 - 1.34

expansion (10) into Eq. (13) yields

$$\mathbb{E}\{X_{t_1}X_{t_2}\} = \sum_{m_1=0}^{\infty}\sum_{m_2=0}^{\infty}\sum_{m_3=0}^{\infty} U_{m_1}\ e^{-p\lambda_{m_1}t_1}\ \mathcal{B}_{m_1,m_2}\ \times \\ e^{-p\lambda_{m_2}(t_2-t_1)}\ \mathcal{B}_{m_2,m_3}\ e^{-p\lambda_{m_3}(t_2-t_1)}\ \tilde{U}^*_{m_3},$$

where

$$\mathcal{B}_{m,m'} = \int_{\Omega} d\mathbf{r}\ u^*_m(\mathbf{r})\ B(\mathbf{r})\ u_{m'}(\mathbf{r}).$$

Using the diagonal matrix $\Lambda_{m,m'}$, the triple sum over m_1, m_2 and m_3 can be written in the compact form of a scalar product:

$$\mathbb{E}\{X_{t_1}X_{t_2}\} = \Big(U\ e^{-p\Lambda t_1}\ \mathcal{B}\ e^{-p\Lambda(t_2-t_1)}\ \mathcal{B}\ e^{-p\Lambda(1-t_2)}\ \tilde{U}^*\Big).$$

Similar expression can be written for the n-point correlation function [6]

$$\mathbb{E}\{X_{t_1}...X_{t_n}\} = \Big(U\ e^{-p\Lambda t_1}\ \mathcal{B}\ e^{-p\Lambda(t_2-t_1)}\ ...\ \mathcal{B}\ e^{-p\Lambda(1-t_n)}\ \tilde{U}^*\Big). \qquad (14)$$

The n^{th}-order moment $\mathbb{E}\{\phi^n/n!\}$ is then given by multiple integration of this expression with the normalized temporal profile $f(t)$:

$$\mathbb{E}\{\phi^n/n!\} = \int_0^1 dt_1\ f(t_1)... \int_{t_{n-1}}^1 dt_n\ f(t_n)\ \mathbb{E}\{X_{t_1}...X_{t_n}\}. \qquad (15)$$

2.4 Simple geometries

To illustrate applications of the multiple correlation function approach, we consider restricted diffusion in simple geometries: a slab, a cylinder, and a sphere. In this case, the Laplace operator eigenbasis is known explicitly [29,30], allowing us to perform the computation analytically. Note also that the inversion symmetry of these domains implies that all odd moments $\mathbb{E}\{\phi^{2n+1}\}$ vanish.

2.4.1 Slab

We start with the case of two parallel infinite planes at distance $2L = 2$ (a slab) when the gradient direction is perpendicular to them. This problem is equivalent to one-dimensional diffusion on the interval $(-1, 1)$. In contrast with Ref. [6], we consider here the symmetric interval to simplify calculations[2]. For convenience, the eigenmodes will be enumerated by double index $m =$

[2] Many results for a symmetric slab can be related to those in Ref. [6] by rescaling the length L by factor 2. So, the dimensionless parameters become: $p = 4p'$, $q =$

Diffusion Fundamentals 5 (2007) 1.1 - 1.34

(nk). The first integer $n \in \{0, 1\}$ distinguishes two sets of eigenfunctions and eigenvalues:

$$\begin{aligned} u_{0k} &= \beta_{0k} \cos(\alpha_{0k} x), \qquad & \lambda_{0k} &= \alpha_{0k}^2, \\ u_{1k} &= \beta_{1k} \sin(\alpha_{1k} x), \qquad & \lambda_{1k} &= \alpha_{1k}^2. \end{aligned}$$

The second index $k = 0, 1, 2...$ enumerates all positive zeros α_{nk} of the functions

$$\begin{aligned} y_0(z) &= z \sin z - h \cos z, \\ y_1(z) &= z \cos z + h \sin z, \end{aligned} \tag{16}$$

representing the boundary condition (9). The normalization constants β_{nk} are

$$\beta_{nk} = \left(\frac{\lambda_{nk} + h^2}{\lambda_{nk} + h(h+1)} \right)^{1/2}.$$

Barzykin computed the matrix $\mathcal{B}$ and the vectors U and $\tilde{U}$ for restricted diffusion between parallel planes in a linear magnetic field gradient with a uniform initial density $\rho_0(\mathbf{r}) = 1/2$ [25]:

$$\begin{aligned} U_{nk} =& \tilde{U}_{nk} = \delta_{n,0} \frac{\sqrt{2}\ h}{\sqrt{\lambda_{0k}(\lambda_{0k} + h(h+1))}}, \\ \mathcal{B}_{nk,n'k'} =& 2\delta_{n,n'\pm 1} \frac{\sqrt{\lambda_{nk}}}{\sqrt{\lambda_{nk} + h(h+1)}} \ \frac{\sqrt{\lambda_{n'k'}}}{\sqrt{\lambda_{n'k'} + h(h+1)}} \ \frac{\lambda_{nk} + \lambda_{n'k'} + 2h^2}{(\lambda_{nk} - \lambda_{n'k'})^2}. \end{aligned} \tag{17}$$

As a result, the numerical computation is completely reduced to finding the positive zeros α_{nk} of the functions $y_0(z)$ and $y_1(z)$ in Eq. (16) that can be implemented in a simple and rapid way.

2.4.2 Cylinder

For an infinite cylinder (or a circle) of unit radius, the classical representation of the eigenfunctions involves two positive indices n and k

$$u_{nk}(r, \varphi) = \frac{\epsilon_n}{\sqrt{\pi}} \ \frac{\beta_{nk}}{J_n(\alpha_{nk})} \ J_n(\alpha_{nk} r) \ \cos(n\varphi),$$

$\overline{q'/2,\ h} = h'/2$, where prime denotes the parameters from Ref. [6]. Note that the expressions for β_{nk}, U_{nk}, $B_{nk,n'k'}$, and other related quantities are also modified due to the shift of the interval.

Diffusion Fundamentals 5 (2007) 1.1 - 1.34

where $J_n(z)$ are the Bessel functions of the first kind. The eigenvalues $\lambda_{nk} = \alpha_{nk}^2$ are expressed through the positive zeros α_{nk} of the functions

$$y_n(z) = z\ J_n'(z) + h\ J_n(z), \tag{18}$$

representing the boundary condition (9). The normalization constants β_{nk} are

$$\beta_{nk} = \left(\frac{\lambda_{nk}}{\lambda_{nk} - n^2 + h^2} \right)^{1/2}.$$

For a linear gradient and uniform initial density $\rho_0(\mathbf{r}) = 1/\pi$, one finds [6]

$$\begin{aligned} U_{nk} =& \tilde{U}_{nk} = \delta_{n,0}\ \frac{2h}{\sqrt{\lambda_{0k}(\lambda_{0k} + h^2)}}, \\ \mathcal{B}_{nk,n'k'} =& \delta_{n,n'\pm1} \Big(1 + \delta_{n,0} + \delta_{n',0}\Big)^{1/2} \beta_{nk}\beta_{n'k'} \frac{\lambda_{nk} + \lambda_{n'k'} - 2nn' + 2h(h-1)}{(\lambda_{nk} - \lambda_{n'k'})^2}. \end{aligned} \tag{19}$$

2.4.3 Sphere

For a sphere of unit radius, the eigenfunctions are

$$u_{nk}(r,\theta) = \frac{1}{\sqrt{2\pi}} \frac{\beta_{nk}}{j_n(\alpha_{nk})}\ j_n(\alpha_{nk} r)\ P_n(\cos\theta),$$

where the third index and the polar coordinate are omitted. Here $P_n(x)$ are the Legendre polynomials, and $j_n(z)$ the spherical Bessel functions

$$j_\nu(z) = (\pi/2z)^{1/2}\ J_{\nu+1/2}(z).$$

The eigenvalues $\lambda_{nk} = \alpha_{nk}^2$ are expressed thourgh the positive zeros of the functions

$$y_n(z) = z\ j_n'(z) + h\ j_n(z), \tag{20}$$

representing the boundary condition (9). The normalization constants β_{nk} are

$$\beta_{nk} = \left(\frac{(2n+1)\lambda_{nk}}{\lambda_{nk} - n(n+1) + h(h-1)} \right)^{1/2}.$$

Diffusion Fundamentals 5 (2007) 1.1 - 1.34

For a linear gradient and uniform initial density $\rho_0(\mathbf{r}) = 3/4\pi$, one finds [6]

$$\begin{aligned} U_{nk} =& \tilde{U}_{nk} = \delta_{n,0}\ \frac{\sqrt{6}\ h}{\sqrt{\lambda_{0k}(\lambda_{0k}+h(h-1))}}, \\ \mathcal{B}_{nk,n'k'} =& \frac{(n+n'+1)\ \delta_{n,n'\pm1}}{(2n+1)\ (2n'+1)}\ \beta_{nk}\ \beta_{n'k'}\times \\ & \frac{\lambda_{nk}+\lambda_{n'k'}-n(n'+1)-n'(n+1)+1+2h(h-2)}{(\lambda_{nk}-\lambda_{n'k'})^2}. \end{aligned} \tag{21}$$

2.5 Explicit relations for the moments

Substituting the above explicit formulas for $\mathcal{B}$, Λ, U and $\tilde{U}$ into the matrix representation (14), one can write correlation functions in an exact and explicit form. So, the reference signal is proportional to

$$\mathbb{E}\{1\} = 2dh^2 \sum_{k=0}^{\infty} \frac{e^{-p\lambda_{0k}}}{\lambda_{0k}(\lambda_{0k}+h(h-d+2))} \tag{22}$$

for three geometries: slab ($d = 1$), cylinder ($d = 2$) and sphere ($d = 3$). Although the structure of this sum is the same for the three confining domains, the sets of the eigenvalues λ_{0k} are different.

Similarly, the two-point correlation function can be written explicitly as

$$\begin{aligned} \mathbb{E}\{X_{t_1}X_{t_2}\} =& 8h^2 \sum_{k_1,k_2,k_3} \frac{e^{-p\lambda_{0k_1}t_1}}{(\lambda_{0k_1}+h(h-d+2))}\ \times \\ & \frac{\lambda_{0k_1}+\lambda_{1k_2}+2h(h-d+1)}{(\lambda_{0k_1}-\lambda_{1k_2})^2}\ \frac{\lambda_{1k_2}\ e^{-p\lambda_{1k_2}(t_2-t_1)}}{\lambda_{1k_2}+(h+1)(h-d+1)}\ \times \\ & \frac{\lambda_{0k_3}+\lambda_{1k_2}+2h(h-d+1)}{(\lambda_{0k_3}-\lambda_{1k_2})^2}\ \frac{e^{-p\lambda_{0k_3}(1-t_2)}}{(\lambda_{0k_3}+h(h-d+2))}, \end{aligned} \tag{23}$$

where the sums over n_1, n_2 and n_3 were reduced to $n_1 = n_3 = 0$ and $n_2 = 1$ due to Kronecker δ-symbols in the relations (17, 19, 21) for the matrix $\mathcal{B}$ and the vector U. Higher-order moments can also be treated in a similar way (see [32] for some related techniques).

It is worth noting that Eqs. (22) and (23) are exact, no simplifying approximations were used. For numerical analysis, one first finds for a given h the positive zeros α_{nk} of the functions $y_n(z)$ given by Eq. (16), (18), or (20), depending on the domain. The asymptotically quadratic growth of the eigenvalues λ_{nk} with k ensures a rapid convergence of the above sums (if p is not too small). Although this computation is simple and accurate, it is not complete (except for the reference signal). For instance, calculation of the second moment

Diffusion Fundamentals 5 (2007) 1.1 - 1.34

$\mathbb{E}\{\phi^2/2\}$ (or any higher-order moment) requires the time average of the correlation function with a given temporal profile $f(t)$ according to Eq. (15). The complete computation may become too lengthy and very time consuming.

This challenge can be overcome in two asymptotic regimes when the dimensionless diffusion coefficient p is small or large with respect to 1. Using the explicit form of Eqs. (22) and (23), one can derive accurate results for both regimes. In the next section, a Laplace transform summation technique is applied to study the slow-diffusion regime $p \ll 1$, while the motional narrowing regime $p \gg 1$ will be considered in Sec. 4. It will be shown that the obtained results are accurate and applicable to a wide range of the parameter p.

3 Slow-diffusion regime

In the slow-diffusion regime $p \ll 1$, a large number of terms has to be taken into account for accurate computation of the moments $\mathbb{E}\{1\}$ and $\mathbb{E}\{\phi^2/2\}$. We start with a simpler case of the zeroth moment to better illustrate the ideas, while the computation of the second moment is given in Appendix.

Since p is small, the asymptotic behavior of $\mathbb{E}\{1\}$ as a function of p could formally be obtained by expanding the exponential function $e^{-p\lambda_{0k}}$ in Eq. (22) in a power series:

$$\mathbb{E}\{1\} \simeq \left(\sum_{k=0}^{\infty} \frac{2dh^2}{\lambda_{0k}(\lambda_{0k} + h(h-d+2))}\right) - p\left(\sum_{k=0}^{\infty} \frac{2dh^2}{\lambda_{0k} + h(h-d+2)}\right) + ...,$$

where the expressions in parentheses would be just coefficients depending on h and d. Although this expansion gives correct asymptotic behavior up to p (see below), the higher-order terms diverge, failing this naive approach.

To overcome this difficulty, it is convenient to perform the Laplace transform of $\mathbb{E}\{1\}$ with respect to p:

$$\mathcal{L}[\mathbb{E}\{1\}](s) = 2dh^2 \sum_{k=0}^{\infty} \frac{1}{\lambda_{0k}(\lambda_{0k} + h(h-d+2))(s+\lambda_{0k})}. \tag{24}$$

As the zeroth moment itself, its Laplace transform is expressed as a sum over eigenvalues λ_{0k}. But the crucial simplification here is that the terms in Eq. (24) are products of simple fractions, without exponential functions. Elementary algebraic transformations reduce this sum to

$$\mathcal{L}[\mathbb{E}\{1\}](s) = \frac{2dh^2}{h(h-d+2)-s}\left(\frac{\eta_0(0)-\eta_0(-h(h-d+2))}{h(h-d+2)} - \frac{\eta_0(0)-\eta_0(-s)}{s}\right), \tag{25}$$

Diffusion Fundamentals 5 (2007) 1.1 - 1.34

where

$$\eta_n(s) \equiv \sum_{k=0}^{\infty} \frac{1}{s - \lambda_{nk}}. \tag{26}$$

Since the eigenvalues λ_{nk} are determined through the zeros of some explicit functions, the summation in Eq. (26) can be performed analytically, as shown below.

3.1 Laplace transform summation technique

The computation of the function $\eta_n(s)$ in Eq. (26) is based on a simple consequence of the Mittag-Leffler theorem in complex analysis [31]. Let $\{z_k\}$ be a sequence of all zeros (with multiplicities $\{m_k\}$) of some entire function $y(z)$ so that it can be written as

$$y(z) = a_0 \prod_k (z - z_k)^{m_k}$$

(here a_0 is a constant). Taking derivative and dividing it by $y(z)$, one formally gets

$$\frac{y'(z)}{y(z)} = \sum_k \frac{m_k}{z - z_k}.$$

In the case of infinite sequence of zeros, this consideration can be made rigorous by requiring that z_k go to infinity, and

$$\sum_k \frac{1}{|z_k|} = \infty. \tag{27}$$

For slab, cylinder, and sphere, the set $\{\pm\alpha_{nk}\}$ contains all the simple zeros z_k (with multiplicities $m_k = 1$) of the entire functions $y_n(z)$ defined by Eq. (16), (18), or (20), depending on the domain. The asymptotic behavior $\alpha_{nk} \propto k$ (for fixed n) implies the divergence of the series in Eq. (27), allowing one to apply the Mittag-Leffler theorem for the computation of the functions $\eta_n(s)$

$$\eta_n(s) = \frac{1}{2\sqrt{s}} \sum_{k=0}^{\infty} \left(\frac{1}{\sqrt{s} - \alpha_{nk}} + \frac{1}{\sqrt{s} + \alpha_{nk}} \right) = \left(\frac{y_n'(z)}{2z\ y_n(z)} - \frac{n}{2z^2} \right)_{z=\sqrt{s}}. \tag{28}$$

Here the last term is subtracted to get rid off the supplementary zero $z = 0$ (with multiplicity n) of the function $y_n(z)$ when $n > 0$. Substitution of Eqs. (16), (18), and (20) into Eq. (28) leads to exact and explicit relations for the function $\eta_n(s)$, e.g.

Diffusion Fundamentals 5 (2007) 1.1 - 1.34

$$\eta_0(s) = \frac{(h-d+2)\psi_d(s)+1}{2(s\psi_d(s)-h)}, \tag{29}$$

$$\eta_1(s) = \frac{(h-d+1)-(s+d(h-d+1))\psi_d(s)}{2s(1+(h-d+1)\psi_d(s))}, \tag{30}$$

where the function $\psi_d(s)$ is defined as

$$\psi_d(s) = \begin{cases} \dfrac{\sin(\sqrt{s})}{\sqrt{s}\ \cos(\sqrt{s})}, & d=1, \\ \dfrac{J_1(\sqrt{s})}{\sqrt{s}\ J_0(\sqrt{s})}, & d=2, \\ \dfrac{j_1(\sqrt{s})}{\sqrt{s}\ j_0(\sqrt{s})}, & d=3. \end{cases} \tag{31}$$

As one will see, many other sums involving the eigenvalues λ_{nk} can be expressed through this function.

3.2 Zeroth moment

Substitution of the explicit function $\eta_0(s)$ in Eq. (25) yields, after algebraic simplifications, the following exact relation:

$$\mathcal{L}[\mathbb{E}\{1\}](s) = \frac{1}{s} - \frac{hd}{s}\ \frac{\psi_d(-s)}{h+s\psi_d(-s)}. \tag{32}$$

The zeroth moment $\mathbb{E}\{1\}$ as a function of p can then be found by the inverse Laplace transform, albeit this operation is difficult in practice. In the limit $h \to 0$, one simply gets $\mathcal{L}[\mathbb{E}\{1\}](s) = 1/s$, and the inverse Laplace transform is equal to 1 as it should be in the case without surface relaxation.

The asymptotic behavior in the slow-diffusion regime $p \to 0$ corresponds to $s \to \infty$. In this limit, the asymptotic behavior of the function $\psi_d(-s)$ is

$$\psi_d(-s) \simeq \begin{cases} s^{-1/2}\Big(1-2e^{-2\sqrt{s}}+...\Big), & d=1, \\ s^{-1/2}\Big(1-s^{-1/2}/2-s^{-1}/8+...\Big), & d=2, \\ s^{-1/2}\Big(1-s^{-1/2}+2e^{-2\sqrt{s}}+...\Big), & d=3. \end{cases} \tag{33}$$

Note that the series expansion for $d=1$ and $d=3$ contains only few terms ($s^{-1/2}$ for $d=1$ and $s^{-1/2}-s^{-1}$ for $d=3$) and exponentially small corrections. In contrast, the series expansion for $d=2$ contains infinite number of polynomial terms. The substitution of these expansions in Eq. (32) yields

$$\mathcal{L}[\mathbb{E}\{1\}] = \frac{1}{s} - \frac{hd}{s^2} + \frac{h^2 d}{s^{5/2}} - \frac{h^2(h-(d-1)/2)d}{s^3} + O(s^{-7/2})\ .$$

Diffusion Fundamentals 5 (2007) 1.1 - 1.34

Using the identity $\mathcal{L}^{-1}[s^{-\beta}] = t^{\beta-1}/\Gamma(\beta)$ with the Euler gamma function $\Gamma(z)$, one finds the zeroth moment in the slow-diffusion regime ($p \ll 1$)

$$\mathbb{E}\{1\} = 1 - hd\ p + \frac{4}{3\sqrt{\pi}}\ h^2 d\ p^{3/2} - \frac{1}{2}h^2(h - (d-1)/2)d\ p^2 + O(p^{5/2})\ . \quad (34)$$

3.3 Second moment

The expression (23) for the correlation function $\mathbb{E}\{X_{t_1}X_{t_2}\}$ contains three exponential functions with different arguments. The triple Laplace transform of this expression with respect to pt_1, $p(t_2 - t_1)$, and $p(1 - t_2)$ yields a cumbersome but still elementary sum (see Appendix A.3). Its terms are products of fractions containing the eigenvalues λ_{nk}. The Laplace transform summation technique can be applied in a similar way as for the zeroth moment, but the computation becomes more lengthy. The main steps of this computation are given in Appendix A.4. The net result is the following:

$$\begin{aligned}\mathbb{E}\{\phi^2/2\} \simeq p < (t_1 - t_2) >_2 + p^{3/2}\frac{4}{3\sqrt{\pi}}\Bigg[< (t_2 - t_1)^{3/2} >_2 + \\ h\Big(< t_2^{3/2} >_2 + < t_1^{3/2} >_2 + < (1 - t_1)^{3/2} >_2 + < (1 - t_2)^{3/2} >_2 \Big)\Bigg] + O(p^2)\end{aligned} \quad (35)$$

where the time averages were defined by Eq. (12). When the Gaussian phase approximation is applicable, this result determines the spin-echo signal attenuation according to Eq. (6) in the slow-diffusion regime ($p \ll 1$).

When the effective temporal profile $f(t)$ is antisymmetric, $f(1 - t) = -f(t)$, the time averages in front of h compensate each other, resulting in the classical expansion [3]

$$\mathbb{E}\{\phi^2/2\} \simeq p < (t_1 - t_2) >_2 + p^{3/2}\frac{4}{3\sqrt{\pi}} < (t_2 - t_1)^{3/2} >_2 + O(p^2). \quad (36)$$

The dependence of the second moment on h appears in higher-order terms. This observation is useful in two opposite situations. On the one hand, if surface relaxation effects should be reduced, the use of antisymmetric temporal profiles is preferable. On the other hand, if slow-diffusion measurements are intended for determination of the surface relaxivity, it is worth to apply

[3] For details, see [6] and references therein. At this point, it is worth recalling that here, in contrast to Ref. [6], L is the half separation length between parallel planes. Due to this distinction, the coefficient in front of $p^{3/2}$ in Eq. (36) is $4/3\sqrt{\pi}$, and not $8/3\sqrt{\pi}$ as in Ref. [6]. At the same time, the results are exactly the same for a cylinder and a sphere.

non-antisymmetric temporal profiles. In this case, the temporal profile can be optimized to increase the contribution of the last term in Eq. (35).

3.4 Temporal profiles

The above results can be applied for arbitrary temporal profile $f(t)$. As an example, we consider the temporal profile consisting of two rectangular pulses of duration δ with $0 < \delta \leq 1/2$ (Fig. 1):

$$f(t) = \Theta(t) - \Theta(t-\delta) - \Theta(t-1/2) + \Theta(t-1/2-\delta), \tag{37}$$

where $\Theta(t)$ is the Heaviside function: $\Theta(t) = 1$ for $t > 0$, and 0 otherwise. Tedious but straightforward calculation yields for any power $\alpha > 0$

$$\begin{aligned} <(t_2-t_1)^\alpha>_2 &= \frac{2\delta^{\alpha+2} + 2(1/2)^{\alpha+2} - (1/2+\delta)^{\alpha+2} - (1/2-\delta)^{\alpha+2}}{(\alpha+1)(\alpha+2)}, \\ <t_1^\alpha>_2 = -<t_2^\alpha>_2 &= \frac{(1/2+\delta)^{\alpha+2} - \delta^{\alpha+2}(\alpha+1) - (1/2)^{\alpha+2}(1+2(\alpha+2)\delta)}{(\alpha+1)(\alpha+2)}. \end{aligned}$$

For example, in the case of a steady bipolar gradient ($\delta = 1/2$), one has

$$\begin{aligned} <(t_1-t_2)>_2 &= \frac{1}{12}, \\ <-(t_2-t_1)^{3/2}>_2 &= \frac{4-\sqrt{2}}{35}, \\ <t_1^{3/2}>_2 = -<t_2^{3/2}>_2 &= \frac{16-7\sqrt{2}}{140}. \end{aligned}$$

When the gradient pulses are very narrow ($\delta \ll 1$), one finds

$$\begin{aligned} <(t_1-t_2)>_2 &= \delta^2(1/2-\delta/3), \\ <-(t_2-t_1)^{3/2}>_2 &\simeq (1/2)^{3/2}\delta^2, \\ <t_1^{3/2}>_2 = -<t_2^{3/2}>_2 &\simeq (1/2)^{5/2}\delta^2. \end{aligned}$$

In general, the time averages can be found by numerical integration with a given profile $f(t)$.

Diffusion Fundamentals 5 (2007) 1.1 - 1.34

4 Motional-narrowing regime

In the motional-narrowing regime ($p \gg 1$), diffusing spins explore the confining domain several times during the experiment. Since the eigenvalues λ_{nk} rapidly grow with k and appear as arguments of exponential functions, the relevant contributions to the related sums correspond to the lowest eigenvalue. For instance, the zeroth moment $\mathbb{E}\{1\}$ can be very accurately approximated by the first term in Eq. (22) with $k = 0$:

$$\mathbb{E}\{1\} \simeq \frac{2h^2 d}{\lambda_{00}(\lambda_{00} + h(h - d + 2))}\, e^{-p\lambda_{00}}. \tag{38}$$

For weak surface relaxation ($h \ll 1$), one can replace λ_{00} by its asymptotic value hd, giving

$$\mathbb{E}\{1\} \simeq e^{-phd}.$$

In the opposite limit of very strong surface relaxation ($h \to \infty$), the lowest eigenvalue approaches a constant λ_{00}^{∞}, so that the zeroth moment tends to

$$\mathbb{E}\{1\} \simeq \frac{2d}{\lambda_{00}^{\infty}} e^{-p\lambda_{00}^{\infty}}.$$

Note that

$$\lambda_{00}^{\infty} = \begin{cases} \pi^2/4 \simeq 2.467401101, & d = 1, \\ \quad\ \simeq 5.783185964, & d = 2, \\ \pi^2 \quad\ \simeq 9.869604404, & d = 3 \end{cases}$$

(for $d = 2$, $\sqrt{\lambda_{00}^{\infty}}$ is the first positive zero of $J_0(z)$).

4.1 Second moment

The analysis of the second moment is more complicated. In Sec. 3, we first computed the correlation function $\mathbb{E}\{X_{t_1} X_{t_2}\}$, found its asymptotic behavior as $p \to 0$, and then took time average according to Eq. (11). When p is large, such a perturbative approach fails since the series expansion of the exponential functions in Eq. (23) is not applicable any more. To overcome this difficulty, it is convenient first to calculate the time average with a chosen temporal profile $f(t)$, and then compute the remaining sum. To illustrate the idea, we consider a steady (bipolar) linear gradient (37) with $\delta = 1/2$, for which a

Diffusion Fundamentals 5 (2007) 1.1 - 1.34

direct computation yields

$$< e^{-p_1 t_1 - p_2(t_2-t_1) - p_3(1-t_2)} >_2 = \frac{2e^{-p_1/2-p_2/2} - 2e^{-p_1/2-p_3/2} + 2e^{-p_2/2-p_3/2} - e^{-p_2}}{(p_2-p_3)(p_2-p_1)} + \frac{e^{-p_1}}{(p_1-p_3)(p_1-p_2)} + \frac{e^{-p_3}}{(p_3-p_1)(p_3-p_2)}, \tag{39}$$

p_i denoting $p\lambda_{n_i,k_i}$ (one can also treat arbitrary duration $0 < \delta < 1/2$). The computation of the remaining sum could be performed in the general case (i.e., for any value of p) by using the Laplace transform summation technique of Sec. 3. The resulting formula is exact but too lengthy for practical use.

When p is large enough, the analysis is much simpler since the relevant contributions come only from the terms containing the lowest eigenvalue λ_{00} (other terms decrease much faster). The technical details of the computation are given in Appendix A.5. The net result for the second moment in the motional-narrowing regime is:

$$\mathbb{E}\{\phi^2/2\} \simeq \left(\frac{\zeta_{-1}(h)}{p} - \frac{3\zeta_{-2}(h)}{p^2} \right) e^{-p\lambda_{00}}, \tag{40}$$

where two coefficients $\zeta_{-1}(h)$ and $\zeta_{-2}(h)$ and the lowest eigenvalue λ_{00} depend both on h and the confining geometry. Their exact formulas and asymptotic expressions are given in Appendix A.5. In the case of a purely reflecting boundary ($h = 0$), one retrieves the classical results derived by Robertson and Neuman [3,7]. It is worth noting that further corrections to Eq. (40) are exponentially small so that this formula is very accurate for large enough p. As discussed in [6], the presence of only two terms p^{-1} and p^{-2} is a specific feature of the steady bipolar temporal profile $f(t)$. In general, one should expect the leading term of order of p^{-1}, while correction terms can be different. In the next section, we discuss the physical consequences of these findings.

5 Discussion

We start by resuming the relevant physical quantities describing the signal attenuation. Three dimensionless parameters were introduced to quantify the gradient strength ($q = \gamma g T L$), the diffusion rate ($p = DT/L^2$), and the surface relaxation ($h = \rho L/D$). Since the total phase is proportional to g, its second moment is always proportional to q^2. When the Gaussian phase approximation (6) is valid, all the nontrivial properties of restricted diffusion reside in the dependence of the moments $\mathbb{E}\{1\}$ and $\mathbb{E}\{\phi^2/2\}$ on the two other parameters, p and h.

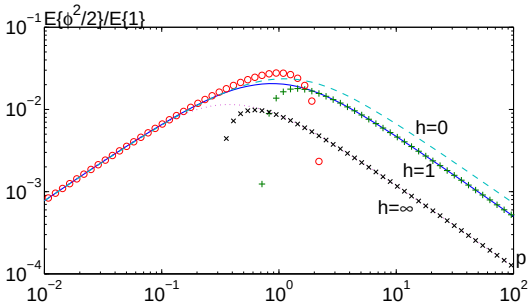

Fig. 2. Normalized second moment $\mathbb{E}\{\phi^2/2\}/\mathbb{E}\{1\}$ as a function of p for a cylinder with $h = 1$: accurate numerical summation (solid line), slow-diffusion regime (36) (circles) and motional-narrowing regime (40) (pluses). For comparison, the normalized second moment with $h = 0$ and $h = \infty$ is shown by dashed and dotted lines, respectively (croses indicate the motional-narrowing approximation for $h = \infty$). Similar behavior is observed for a slab and a sphere (not shown).

5.1 Normalized second moment

Figure 2 shows the normalized second moment $\mathbb{E}\{\phi^2/2\}/\mathbb{E}\{1\}$ as a function of p for a cylinder for different values of h. The obtained $\cap$-shape is well known for the case without surface relaxation ($h = 0$). When the nuclei diffuse slowly ($p \ll 1$), their dephasing is small and the consequent signal attenuation is weak (left branch of the curve). In the opposite limit $p \gg 1$, the nuclei diffuse very fast so that magnetic field inhomogeneities are averaged out, making the variables X_{t_1} and X_{t_2} be almost uncorrelated. As a consequence, the correlation function $\mathbb{E}\{X_{t_1}X_{t_2}\}$ is small (right branch of the curve). When the diffusion length $\sqrt{DT}$ is comparable to the size L of confinement (i.e., $p \sim 1$), the second moment reaches its maximum, yielding the strongest signal attenuation (at fixed gradient intensity). It is important to stress that this $\cap$-shape appears for any value of the dimensionless surface relaxivity h.[4] Similar behavior is found for a slab and a sphere (not shown).

As one can see, the slow-diffusion approximation (36) and the motional-narrowing approximation (40) provide very accurate description of the normalized second moment for small and large p, respectively. Moreover, their domains of applicability extend almost to $p = 1$.

In the slow-diffusion regime, the normalization by $\mathbb{E}\{1\}$ can lead only to corrections of order of p^2 or higher:

$$\mathbb{E}\{\phi^2/2\}/\mathbb{E}\{1\} \simeq \mathbb{E}\{\phi^2/2\} + O(p^2) \quad (p \ll 1).$$

[4] This result is in contradiction with Figure 2 of Ref. [27], on which the signal exhibited a second minimum corresponding to a second maximum of the normalized second moment within GPA. But the condition for the magnetization survival up to the echo time was not taken into account in [27].

As the second moment itself, this expression is independent of h up to the order $p^{3/2}$. It is important to stress, however, that the slow-diffusion approximation (36) is applicable only for relatively small h. When h is large enough, higher-order corrections in p can become dominant. To illustrate this idea, let us consider again the Laplace transform (32) of the zeroth moment $\mathbb{E}\{1\}$. In the limit $h \to \infty$, one has

$$\lim_{h\to\infty} \mathcal{L}[\mathbb{E}\{1\}](s) = \frac{1}{s} - d\frac{\psi_d(-s)}{s}.$$

Its expansion for large s and the inverse Laplace transform yields

$$\lim_{h\to\infty} \mathbb{E}\{1\} \simeq 1 - p^{1/2}\frac{2d}{\sqrt{\pi}} + O(p).$$

Note that the term $p^{1/2}$ was not present in Eq. (34). This relation is applicable when $p \ll 1$ and $h \gg 1/p$. Surprisingly, in spite of this modification, the normalized second moment is well represented by Eq. (36) even for very high values of h (see Fig. 2).

In contrast, the normalization of the second moment by $\mathbb{E}\{1\}$ becomes important for the motional-narrowing regime. In fact, both the zeroth and second moments exponentially decay for large p due to the factor $e^{-p\lambda_{00}}$. Only when h is strictly equal to 0, this factor vanishes as λ_{00} becomes 0. What is remarkable that the exponential function $e^{-p\lambda_{00}}$ is factored out when the diffusion-weighted signal is normalized by the reference signal, resulting in a polynomial decay of the normalized second moment as p goes to infinity:

$$\frac{\mathbb{E}\{\phi^2/2\}}{\mathbb{E}\{1\}} \simeq \frac{\zeta'_{-1}(h)}{p} - \frac{3\zeta'_{-2}(h)}{p^2},$$

where

$$\zeta'_{-k}(h) = \zeta_{-k}(h)\frac{\lambda_{00}(\lambda_{00} + h(h-d+2))}{2h^2 d}.$$

This is a specific feature of the rapid diffusion when each nucleus travels long distances, exploring the whole confining domain. In this case, all the nuclei are affected by surface relaxation in a more or less similar way, and the exponential decay of their magnetization is already represented by the zeroth moment $\mathbb{E}\{1\}$. The same exponential factor appears in the second moment, while more subtle (polynomial) modifications are described by the coefficients ζ_{-1} and ζ_{-2} shown in Fig. 3. In other words, although surface relaxation yields spatially inhomogeneous attenuation, its effect is averaged out by rapid diffusion of the nuclei. On the other hand, the exploration of the motional-narrowing regime ($p \gg 1$) in the present of strong surface relaxation ($h \gg 1$) is mostly inaccessible in experiments since the reference and diffusion-weighted signals are both small due to the exponential factor in Eqs. (38) and (40).

Diffusion Fundamentals 5 (2007) 1.1 - 1.34

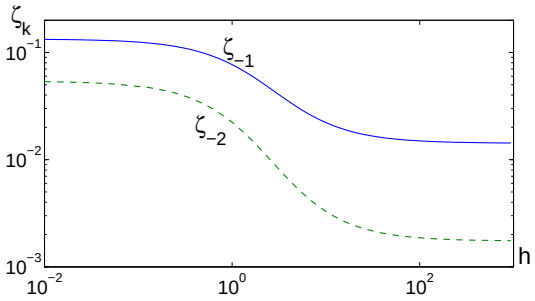

Fig. 3. The coefficients ζ_{-1} and ζ_{-2} as functions of the dimensionless surface relaxivity h for a slab ($d = 1$). Similar behavior is observed for a cylinder and a sphere (not shown).

5.2 Time-dependent or apparent diffusion coefficient

If the Gaussian phase approximation holds, the effect of geometrical confinement can be seen as effective "slowing" down of the diffusive motion by reflections on the boundary. In other words, the signal attenuation due to restricted diffusion can formally be understood as an equivalent signal attenuation due to free (unrestricted) diffusion but with a time-dependent or apparent diffusion coefficient (ADC). In this case, Hahn formula (1) can be written for arbitrary temporal profile as [6]

$$E \propto \exp\Big[-D(T)\ \gamma^2 g^2 T^3 < (t_1 - t_2) >_2\Big]$$

(for a steady bipolar profile, the time average $< (t_1 - t_2) >_2$ is equal to $1/12$). Comparing this expression with Eq. (6), one can relate the ADC to the normalized second moment:

$$\frac{D(T)}{D} \simeq \frac{\mathbb{E}\{\phi^2/2\}/\mathbb{E}\{1\}}{p\ \ < (t_1 - t_2) >_2}.$$

One can thus translate the above results for the normalized second moment in terms of ADC.

5.3 The lowest eigenvalue of the Laplace operator

In the motional-narrowing regime, the reference signal (zeroth moment $\mathbb{E}\{1\}$) and the diffusion-weighted signals (second moment $\mathbb{E}\{\phi^2/2\}$) are completely determined by four parameters: p, h, d, and the lowest eigenvalue λ_{00} of the Laplace operator. This eigenvalue is the only implicit parameter that has to be calculated as a function of h. For any bounded domain with a smooth boundary, λ_{00} is an analytic monotonously increasing function of h, varying from 0 (at $h = 0$, Neumann boundary condition) to some constant (at $h = \infty$,

Diffusion Fundamentals 5 (2007) 1.1 - 1.34

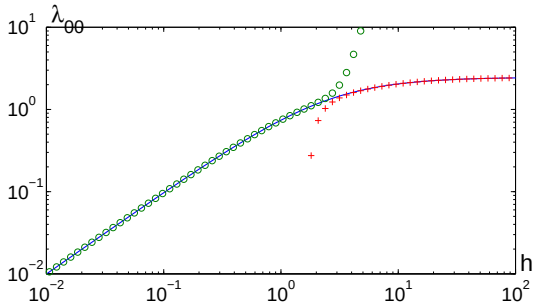

Fig. 4. The lowest eigenvalue λ_{00} of the Laplace operator in a slab ($d = 1$) as a function of the dimensionless surface relaxivity h (solid line) and its truncated series expansions (A.13) and (A.14) at small h (circles) and large h (pluses), respectively. Similar behavior is observed for a cylinder and a sphere (not shown).

Dirichlet boundary condition).

We remind that $\lambda_{00} = \alpha_{00}^2$, where α_{00} is the first positive zero of some explicit function $y_0(z)$ given by Eq. (16), (18), or (20) for a slab, a cylinder, and a sphere, respectively. Using the properties of this function, one can calculate the asymptotic behavior of the lowest eigenvalue in both limits, $h \to 0$ and $h \to \infty$ (see Appendix A.5). For a slab, Fig. 4 shows the eigenvalue λ_{00} as a function of the dimensionless surface relaxivity h. One can see that its truncated series expansions (A.13) and (A.14) provide very accurate approximations at small and large h, respectively. Similar behavior is observed for a cylinder and a sphere.

6 Conclusions

In this paper, we considered restricted diffusion of the nuclei under a linear magnetic field gradient in simple confining domains (slab, cylinder, and sphere) in the presence of surface relaxation. The macroscopic spin-echo signal as a function of the normalized gradient intensity (parameter q) was proportional to the characteristic function of the random dephasing ϕ of an individual nucleus. According to the multiple correlation function approach, the moments of this random variable were expressed in terms of two governing matrices $\mathcal{B}$ and Λ defined through the Laplace operator eigenbasis.

It is worth noting the crucial points allowed us to obtain exact and explicit relations for the zeroth and second moments:

(1) The internal symmetries of the three considered geometries led to explicit representation of the matrix $\mathcal{B}$ in terms of the Laplace operator eigenvalues only. Performing the Laplace transforms, any moment $\mathbb{E}\{\phi^n/n!\}$ can be written as a multiple sum of products of fractions containing the

Diffusion Fundamentals 5 (2007) 1.1 - 1.34

eigenvalues.

(2) The eigenvalues are related to the zeros of explicitly known analytic functions. Using the Laplace transform summation technique, the above multiple sums can be expressed through the only function $\psi_d(s)$ and its derivatives.

(3) A technical point is that all the derivatives of the function $\psi_d(s)$ can be expressed through $\psi_d(s)$ itself. As a consequence, all the quantities of interest can be expressed through $\psi_d(s)$, allowing automated procedure for their symbolic computation.

Several physical consequences were deduced. In the slow-diffusion regime, the second moment expansion in half-integer powers of the dimensionless diffusion coefficient p was calculated up to the power $p^{3/2}$. For antisymmetric temporal profiles, the first two terms of this expansion (p and $p^{3/2}$) were found to be independent of the dimensionless surface relaxivity h (this dependence appeared in terms p^2 and higher), in agreement with the classical results. The condition $f(1-t) = -f(t)$ would thus be preferable to diminish the effect of surface relaxation on measurements of the time-dependent diffusion coefficient $D(t)$. If this condition is not satisfied, the surface relaxivity appeared in the term of order $p^{3/2}$. The use of non-antisymmetric temporal profiles would then be preferable to extract the surface relaxivity ρ from the short-time asymptotic behavior of $D(t)$.

In the motional-narrowing regime, surface relaxation led to an exponential decay of the reference and diffusion-weighted signals as functions of p. The decay rate was determined by the lowest eigenvalue λ_{00} of the Laplace operator which was strictly positive for any $h > 0$. In contrast, the normalized second moment exhibited only polynomial decrease with p, as in the classical case without surface relaxation. Its dependence on h was represented by two coefficients $\zeta_{-1}(h)$ and $\zeta_{-2}(h)$ which were explicitly computed for simple geometries: slab, cylinder, and sphere. The obtained asymptotic expansions in the slow-diffusion and motional-narrowing regimes provided accurate approximation for the second moment even for strong surface relaxation. Higher-order moments can in principle be treated in a similar way, but a systematic computational technique is required to operate efficiently with multiple sums and integrals.

Acknowledgments

This work has been supported by the ANR project "MIPOMODIM n°NT05-1_42030".

A Laplace transform summation technique

Simple algebraic dependences (17, 19, 21) of the matrix elements $\mathcal{B}_{nk,n'k'}$ on the eigenvalues λ_{nk} for three simple geometries (slab, cylinder, sphere) imply that any correlation function $\mathbb{E}\{X_{t_1}...X_{t_n}\}$ can be written as a sum of products of fractions containing the eigenvalues. Using the Laplace transform summation technique, one can reduce the computation of these sums to explicit algebraic relations. In this Appendix, we illustrate this technique by computing and analyzing the second moment.

A.1 Basic summation formulas

The computation is based on a simple fact that the sum

$$\Theta_n^{(j)}(s_1,...,s_j) \equiv \sum_{k=0}^{\infty} \frac{1}{s_1-\lambda_{nk}} \ ... \ \frac{1}{s_j-\lambda_{nk}}$$

can be recurrently reduced to

$$\eta_n(s) \equiv \sum_{k=0}^{\infty} \frac{1}{s-\lambda_{nk}}$$

by a simple algebraic transformation:

$$\Theta_n^{(j)}(\xi_1,...,\xi_j) = \frac{\Theta_n^{(j-1)}(\xi_1,...,\xi_{j-1}) - \Theta_n^{(j-1)}(\xi_1,...,\xi_j)}{\xi_j - \xi_{j-1}}.$$

Starting from $\Theta_n^{(1)}(\xi) \equiv \eta_n(\xi)$, one gets

$$\begin{aligned}
\Theta_n^{(2)}(\xi_1,\xi_2) &= \frac{\eta_n(\xi_1)-\eta_n(\xi_2)}{\xi_2-\xi_1}, \\
\Theta_n^{(3)}(\xi_1,\xi_2,\xi_3) &= \frac{1}{\xi_3-\xi_2}\left(\frac{\eta_n(\xi_1)-\eta_n(\xi_2)}{\xi_2-\xi_1} - \frac{\eta_n(\xi_1)-\eta_n(\xi_3)}{\xi_3-\xi_1}\right), \\
\Theta_n^{(4)}(\xi_1,\xi_2,\xi_3,\xi_4) &= \frac{1}{\xi_4-\xi_3}\left(\frac{1}{\xi_3-\xi_2}\left[\frac{\eta_n(\xi_1)-\eta_n(\xi_2)}{\xi_2-\xi_1} - \frac{\eta_n(\xi_1)-\eta_n(\xi_3)}{\xi_3-\xi_1}\right] - \right. \\
&\quad \left. - \frac{1}{\xi_4-\xi_2}\left[\frac{\eta_n(\xi_1)-\eta_n(\xi_2)}{\xi_2-\xi_1} - \frac{\eta_n(\xi_1)-\eta_n(\xi_4)}{\xi_4-\xi_1}\right]\right).
\end{aligned}$$

Differentiation of these relations with respect to the variables ξ_1, ..., ξ_j further extends the class of analytically computable sums.

Diffusion Fundamentals 5 (2007) 1.1 - 1.34

A.2 Application to slab, cylinder, and sphere

As one will see in the next subsections, the computation of the second moment can be reduced to algebraic expressions containing the functions $\eta_0(s)$ and $\eta_1(s)$ and their multiple derivatives. For three basic geometries, these functions were related by Eqs. (29) and (30) to the function $\psi_d(s)$ depending only on the space dimension d. Moreover, the derivative $\psi'_d(s)$ can also be expressed in terms of $\psi_d(s)$ itself:

$$\psi'_d(s) = \frac{1}{2s} - d\frac{\psi_d(s)}{2s} + \frac{\psi_d^2(s)}{2}.$$

As a result, any algebraic sum over the eigenvalues λ_{0k} and λ_{1k} can be expressed through the function $\psi_d(s)$. This is a crucial computational simplification allowing an automated symbolic analysis. The following properties of the function $\psi_d(s)$ are useful:

$$\begin{aligned}
\psi_d(s) \simeq & \frac{1}{d} - \frac{s}{d^2(d+2)} + \frac{2s^2}{d^3(d+2)(d+4)} + O(s^3) \quad (s \to 0), \\
\psi_d(\lambda_{0k}) = & \frac{h}{\lambda_{0k}}, \qquad \psi_d(\lambda_{1k}) = \frac{-1}{h-d+1}.
\end{aligned}$$

In general, one can use the recurrent relations between Bessel functions (or spherical Bessel functions in 3D) to express any function $\eta_n(s)$ with $n > 0$ through $\psi_d(s)$:

$$\eta_n(s) = \frac{(h-n-d+2) - \Big[s + (2n+d-2)(h-n-d+2)\Big]\psi_d^{(n)}(s)}{2s\Big[1 + (h-n-d+2)\psi_d^{(n)}(s)\Big]}, \quad \text{(A.1)}$$

where the function $\psi_d^{(n)}(s)$ can be defined by the following recurrent relation for $n \geq 1$

$$\psi_d^{(n+1)}(s) \equiv \frac{2n+d-2}{s} - \frac{1}{s\ \psi_d^{(n)}(s)},$$

and $\psi_d^{(1)}(s) \equiv \psi_d(s)$. Note that the functions $\eta_n(s)$ with $n > 1$ are not defined for $d = 1$ so that Eq. (A.1) is useless in this case.

A.3 Computation of the triple sum

If one introduces

$$\tilde{p}_1 = pt_1, \qquad \tilde{p}_2 = p(t_2 - t_1), \qquad \tilde{p}_3 = p(1 - t_2), \qquad \text{(A.2)}$$

Diffusion Fundamentals 5 (2007) 1.1 - 1.34

the triple Laplace transform of the correlation function in Eq. (23) with respect to these variables becomes

$$\mathcal{L}^3[\mathbb{E}\{X_{t_1}X_{t_2}\}](s_1,s_2,s_3) = 8h^2 \sum_{k_1,k_2,k_3} \frac{1}{(\lambda_{0k_1}+h(h-d+2))(s_1+\lambda_{0k_1})} \times \frac{\lambda_{0k_1}+\lambda_{1k_2}+2h(h-d+1)}{(\lambda_{0k_1}-\lambda_{1k_2})^2} \frac{\lambda_{1k_2}}{\lambda_{1k_2}+(h+1)(h-d+1)} \times \frac{1}{s_2+\lambda_{1k_2}} \frac{\lambda_{0k_3}+\lambda_{1k_2}+2h(h-d+1)}{(\lambda_{0k_3}-\lambda_{1k_2})^2} \frac{1}{(s_3+\lambda_{0k_3})(\lambda_{0k_3}+h(h-d+2))}.$$

This expression can be written as

$$\mathcal{L}^3[\mathbb{E}\{X_{t_1}X_{t_2}\}](s_1,s_2,s_3) = 8h^2 \sum_{k_2=0}^{\infty} \mathcal{S}(s_1,\lambda_{1k_2}) \frac{\lambda_{1k_2}}{\lambda_{1k_2}+(h+1)(h-d+1)} \frac{1}{s_2+\lambda_{1k_2}} \mathcal{S}(s_3,\lambda_{1k_2}), \quad \text{(A.3)}$$

where

$$\mathcal{S}(s,\lambda) \equiv \sum_{k=0}^{\infty} \frac{1}{(\lambda_{0k}+h(h-d+2))(s+\lambda_{0k})} \left(\frac{1}{\lambda_{0k}-\lambda} + \frac{2(\lambda+h(h-d+1))}{(\lambda_{0k}-\lambda)^2} \right). \quad \text{(A.4)}$$

Using the summation formulas of Sec. A.1, one gets

$$\mathcal{S}(s,\lambda) = -\left(\Big[1 + 2\Big(\lambda + h(h-d+1)\Big)\partial_{\xi_3} \Big] \Theta_0^{(3)}(-\alpha,-s,\xi_3) \right)_{\xi_3=\lambda},$$

where $\alpha = h(h-d+2)$, and ∂_{ξ_3} denotes the partial derivative with respect to ξ_3. Tedius but straightforward computation yields

$$\mathcal{S}(s,\lambda) = \frac{1}{\lambda}\left(\sigma_0(s) + \frac{\sigma_1(s)}{s+\lambda} + \frac{\sigma_2(s)}{(s+\lambda)^2} \right),$$

where

$$\sigma_0(s) = \frac{\psi_d(-s)}{2h(h+s\psi_d(-s))},$$
$$\sigma_1(s) = \frac{(s+2(h-d+1))\psi_d(-s)+h+3}{2(h+s\psi_d(-s))},$$
$$\sigma_2(s) = -\frac{s(1+(h-d+1)\psi_d(-s))}{(h+s\psi_d(-s))}.$$

We stress again that the computation is mainly based on the algebraic form of the sum (A.4). In turn, the geometry is specified by choosing the appropriate function $\psi_d(s)$.

Diffusion Fundamentals 5 (2007) 1.1 - 1.34